Cordierite II: the role of CO2 and H2O

2 authors:

Boris Kolesov
Russian Academy of Sciences
149 PUBLICATIONS   **2,442** CITATIONS

SEE PROFILE

Charles A. Geiger
University of Salzburg
239 PUBLICATIONS   **4,200** CITATIONS

SEE PROFILE

Some of the authors of this publication are also working on these related projects:

Project   Solid State Li-Ion Conductors View project

Project   Nitrogenous Biosignatures and Implications for Astrobiology View project

Cordierite II: The role of CO_2 and H_2O

B.A. KOLESOV[1] AND C.A. GEIGER[2,*]

[1]Institute of Inorganic Chemistry, Lavrentiev prosp. 3, Novosibirsk 630090, Russia
[2]Institut für Geowissenschaften, Universität Kiel, Olshausenstrasse 40, 24098 Kiel, Germany

ABSTRACT

Polarized single-crystal Raman spectra at room temperature and 5 K and polarized infrared spectra at room temperature were obtained from four natural cordierites of different compositions in the wave number region of the CO_2 symmetric stretching vibration and the H_2O stretching vibrations. The CO_2 molecules are preferentially aligned parallel to the X axis, consistent with results from X-ray diffraction and optical studies. The CO_2 contents of six natural cordierites, previously studied by powder IR methods (Vry et al. 1990), were determined via Raman spectroscopy. A linear relationship was found between CO_2 content and the Raman intensity ratio of the normalized CO_2 stretching mode against a Si-O stretching mode. This permits a determination of the CO_2 contents in cordierite using micro-Raman measurements. The internal stretching modes between 3500 and 3800 cm^{-1} were assigned to various types of H_2O molecules occurring in the channel cavity. Three different orientations of H_2O molecules that have no interactions with alkali cations located at 0,0,0 in the six-membered tetrahedral rings are classified in a static model as Class I H_2O molecules. The H$^{..}$H vector for two of them is parallel to [001], and their molecular planes lie in the XZ and YZ crystal planes. The third type has its H$^{..}$H vector directed along the X axis and its molecular plane lies in the XZ plane. Two other types of H_2O have interactions with the alkali cations located at 0,0,0. They are classified as Class II H_2O. They distinguish themselves by the number of H_2O molecules bonded to the alkali atoms. The formation of weak hydrogen bonds at low temperatures may explain the appearance of some Raman stretching modes below 200 K. The H_2O molecules of Class I-Type I/II are probably dynamically disordered about [001] hopping between orientations in the XY and XZ planes down to 5 K. Class II H_2O may also be disordered, but more measurements are required to describe its dynamic behavior.

INTRODUCTION

The incorporation and orientation of molecular CO_2 and H_2O in the channel cavities of cordierite, $(Mg,Fe)_2Al_4Si_5O_{18}$·X(H_2O, CO_2) were investigated using various experimental and computational methods including DTA and dehydration studies (Sugiura 1959), X-ray and neutron diffraction (e.g., Cohen et al. 1977; Armbruster 1985), IR spectroscopy (Farrell and Newnham 1967; Goldman et al. 1977; Vry et al. 1990), proton NMR spectroscopy (Carson et al. 1982), quasi-elastic neutron scattering (Winkler et al. 1994b), and quantum mechanical calculations (Winkler et al. 1994a). These various studies show that CO_2 is aligned parallel to the X axis of cordierite (Armbruster and Bloss 1982; Armbruster and Bürgi 1982; Aines and Rossman 1984; Armbruster 1985). The behavior of H_2O is more complicated. Farrell and Newnham (1967) found that the H_2O molecules lie in the XZ crystal plane (010) with the H$^{..}$H direction parallel to the channel axis [001]. Goldman et al. (1977), following upon the work of Wood and Nassau (1967) in beryl, concluded that two types of H_2O molecules can be identified, which they labeled as Type I and II. The molecular plane of both Type I and II H_2O is located in the YZ crystal plane (100), but they differ in the orientation of their H$^{..}$H vectors, which are either parallel (Type I) or perpendicular (Type II) to [001]. The apparent discrepancy over the orientation of the H_2O molecular plane proposed by Farrell and Newnham (1967) vs. Goldman et al. (1977) can be explained by the different crystal settings used by the two groups. From neutron diffraction results, Cohen et al. (1977) proposed that the H_2O molecules are statistically disordered over four different orientations with their molecular plane nearly parallel to the XY crystal plane (001). Hochella et al. (1979) proposed, using X-ray methods and a reinterpretation of the neutron diffraction data, that the molecular plane of H_2O is tilted about 29° from (100). Winkler et al. (1994b) proposed that Type I H_2O in synthetic Mg-cordierite is rotationally disordered about [001] and that a pure static description is inappropriate to describe its behavior in the channel cavity. They proposed a two orientation jump model in which the H$^{..}$H vector remains parallel to [001] and the H_2O molecule rotates about its center of mass with an estimated jump time of about 6 ps at room temperature. There is no information on the dynamics of Type II H_2O.

Infrared spectroscopy is a powerful method for the detection and description of H_2O. However, unexplained inconsistencies or problems exist regarding the band assignments for Type I H_2O. In the case of cordierite it was shown that the interaction between H_2O and the silicate framework is very weak (Langer and Schreyer 1976; Winkler et al. 1994a).

*E-mail: nmp46@rz.uni-kiel.de

Goldman et al. (1977) reported ν_1 and ν_3 mode energies for Type I H_2O at ~3650 and 3689 cm^{-1}, respectively. However, the wave numbers of ν_1 and ν_3 of free H_2O in solid inert matrixes are well known. They occur at 3634.5 and 3726.9 cm^{-1} in solid nitrogen (Nelander 1985; Fredin et al. 1977), 3619 and 3733 cm^{-1} in solid argon (Redington and Milligan 1962), and 3633.6 and 3731.7 cm^{-1} in solid oxygen (Tso and Lee 1984). The difference in wave numbers between the two is about 100 cm^{-1}. First principle calculations on the H_2O molecule also give a difference of about 100 cm^{-1}. Thus, it is unclear why the proposed difference between ν_1 and ν_3 of Type I H_2O in cordierite (~40 cm^{-1}) is so small. The wave number difference, $\Delta\nu$, between ν_3 and ν_1 of Type II H_2O is 58 cm^{-1}, which is also small. Here, however, the H_2O interacts with an alkali metal (K, Na) located at 0,0,0 in the center of six-membered rings and, therefore, need not have $\Delta\nu$ of a free H_2O molecule. In addition to this discrepancy, the IR spectra presented by Farrell and Newnham (1967) and Goldman et al. (1977) contain two additional modes at ~3710 and ~3600 cm^{-1} that were not considered in their spectral analysis and band assignments. It is not clear what they represent.

Here we investigate the CO_2 and H_2O molecules in natural cordierites of different $Fe^{2+}/(Mg + Fe^{2+})$ ratios and in a sample with substantial channel alkali cations using polarized single-crystal Raman spectroscopy and polarized IR spectroscopy. Raman and IR spectroscopy, together, give a nearly complete picture of the vibrational behavior (polarizability tensor and dipole momentum) of CO_2 and H_2O in the cavities of cordierite. For the case of CO_2, the polarization direction of the asymmetric ν_3 mode in the IR or symmetric ν_1 mode in the Raman gives the orientation of the CO_2 molecular axis. A determination of the orientation of the H_2O molecule and an assignment of the different internal vibrations is straightforward when both types of spectroscopic data are used and when information on the known energies of vibration of a free H_2O molecule are considered. In both the Raman and IR all internal H_2O vibrations are active. In the IR the polarization of the asymmetric stretch, ν_3, gives the direction of the H··H vector directly, while the polarization of the symmetric stretch, ν_1, gives the orientation of the molecular plane. However, this is difficult in practice, because ν_1 is not strong in the IR. Thus additional information from the Raman active modes is needed. Here ν_3 is weak, but ν_1 is stronger. In Raman spectroscopy one should know independently the α_{xx}, α_{yy}, and α_{zz} polarizabilities along the H_2O axes of the molecule. Then the intensity of the ν_1 mode can be measured for the various crystallographic directions in cordierite and the orientation of H_2O in the channel cavities determined.

A description and an understanding of the role of both molecules in cordierite pertains to the energetics and structural interactions between guest molecules and porous host phases of a variety of structures. Such information is needed in petrologic investigations of the composition of the fluid phase present during metamorphism (e.g., Vry et al. 1990). Laboratory determinations of the H_2O and CO_2 contents of synthetic Mg-cordierite as a function of P and T (e.g., Johannes and Schreyer 1981; Le Breton and Schreyer 1993) have met with mixed success. Raman spectroscopy offers the possibility to better character-ize H_2O and CO_2 in cordierite, because it can be used to determine both their amounts and orientation and at a high spatial resolution with relatively little sample preparation. However, only through a combined use of different spectroscopic methods can a complete description of H_2O in cordierite be made.

EXPERIMENTAL METHODS

Four cordierite samples were chosen for detailed study and six more for the determination of their CO_2 contents. The detailed study includes two Mg-rich samples—one from Madagascar and one nearly end-member Mg-cordierite probably from Sri Lanka. (The samples are from the study of Shannon et al. 1992 and have the labels 56163-90 and 56163-92, respectively, G.R. Rossman, personal communication.) The third sample is an Fe-rich cordierite from Dolni Bory in the Czech Republic (TUB-1 from the TU-Berlin collection) and the fourth an alkali-rich cordierite from Haddam, Connecticut, U.S.A. (an X-ray single-crystal refinement of this Haddam cordierite is given in Armbruster 1986). Compositions as determined by electron microprobe are in Table 1. The six samples used here just for CO_2 determination using Raman methods are the same cordierites used in an IR investigation by Vry et al. (1990) and are described in their Table 1 (Nos. 3, 10, 12, 25, 27, and 32). All samples are low cordierite, space group $Cccm$ with a = 17.7, b = 9.7, and c = 9.3 Å.

Polarized single-crystal Raman spectra were recorded with a Triplemate, SPEX spectrometer with a CCD detector, model LN-1340PB, from Princeton Instruments. The 488 nm and 514 nm lines of an Ar-laser were used for excitation. The spectra at

TABLE 1. Chemical composition of cordierites

Sample Location	TUB-1 Dolni Bory†	TA-1 Haddam‡	RS-1* Madagascar§	RS-2* Sri Lanka‖
Oxide wt%				
SiO$_2$	45.34	48.13	49.48	50.61
TiO$_2$	0.02	0.01	0.00	0.01
Al$_2$O$_3$	32.11	31.14	33.52	34.15
MgO	2.23	8.69	11.43	13.38
FeO	16.89	6.51	3.73	0.83
MnO	0.79	0.39	0.16	0.01
CaO	0.05	0.01	0.00	0.00
K$_2$O	0.00	0.01	0.02	0.00
Na$_2$O	0.56	1.49	0.20	0.17
Total	97.99	96.38	98.54	99.16
Cations				
Si	4.91	5.05	4.98	4.99
Al	4.10	3.85	3.98	3.97
Σ (tet.)	9.01	8.90	8.96	8.96
Mg	0.36	1.84	1.72	1.97
Fe^{2+}	1.53	0.22	0.31	0.07
Mn^{2+}	0.07	0.04	0.01	0.00
Σ (oct.)	1.96	2.10	2.04	2.04
Na	0.12	0.30	0.04	0.03
K	0.00	0.00	0.00	0.00
Σ (channel)	0.12	0.30	0.04	0.03
Fe^{2+} mole fraction				
Fe^{2+}/(Fe^{2+}+Mg)	0.84	0.12	0.16	0.03

Note: Calculated on the basis of 18 oxygens per anhydrous formula unit.
* Analyses from Shannon et al. (1992).
† Granitic pegmatite.
‡ Pegmatite.
§ Metamorphic.
‖ Location uncertain, probably metamorphic.

room temperature were obtained in back-scattering geometry using a conventional micro Raman setup. The laser beam was focused to a diameter of 2 micrometers using a LD-EPIPLAN, 40/0.60 pol., Zeiss objective with a numerical aperture of 0.6. The spectral slit was 5 cm⁻¹. The spectra at low temperatures were obtained in a 90° scattering geometry, where the crystal was fixed onto a cold finger of a helium cryostat (APD Cryogenic Inc., model LT-3-110). The low-temperature experiments were made with a spectral slit of 2 cm⁻¹. The spectra are characterized by a simplified Porto's notation, where the first symbol gives the polarization direction of the incident light and the second one the polarization direction of the scattered light.

The polarized single-crystal infrared measurements were made on the Sri Lanka cordierite at room temperature. A Bruker IFS 66V/S spectrometer with a microscope attachment was used. Thin oriented crystal platelets of 25 μm thickness were prepared, because of the strong absorption given by the H_2O stretching vibrations. Measurements were made along the directions of the three crystal axes with 512 scans at a spectral resolution of 2 cm⁻¹.

RESULTS AND DISCUSSION

The orientation and concentration of CO_2 in cordierite

The intensity of the CO_2 stretching mode at 1383 cm⁻¹ as a function of crystal orientation (Fig. 1) shows that the CO_2 in the channel cavities is preferentially aligned parallel to the X
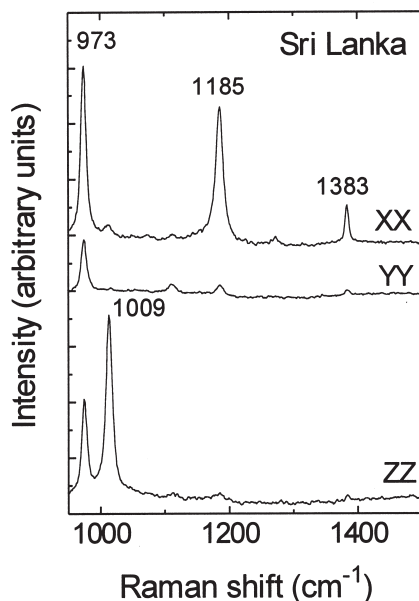
FIGURE 1. Polarized single-crystal Raman spectra of Sri Lanka cordierite at room temperature showing the symmetric CO_2 stretching vibration at 1383 cm⁻¹. For a free gaseous CO_2 molecule it occurs at about 1387 cm⁻¹. The other bands at lower energies are lattice vibrations from the cordierite framework.

axis. The spectra of the Madagascar sample (not shown) are very similar. (The CO_2 contents of the Dolni Bory and Haddam samples are undetectable spectroscopically.) The observed intensities I_{XX}, I_{YY}, and I_{ZZ} are about 800, 140, and 50 arbitrary units, respectively. The polarization leakage was calculated from the numerical aperture of the objective and is about 30 arbitrary units for the I_{YY} and I_{ZZ} spectra. The band at 1383 cm⁻¹ is not a pure CO_2 stretching mode, but one of two components of a Fermi-doublet and this may give rise to mode intensity in an "improper" direction. Hence, we normalize the intensities of I_{YY} to 90 and I_{ZZ} to 0 arbitrary units. From this analysis, only a small fraction of the CO_2, less than 10%, may be parallel to the Y axis, but this estimate is at the limit of experimental uncertainty (Fig. 1). This Raman spectroscopic-based interpretation is consistent with the X-ray diffraction and optical results of Armbruster (1985) and the IR spectra of Aines and Rossman (1984). This orientation is energetically favored because the cavity size is longer in the X-axis direction compared to the Y-axis direction (e.g., Hochella et al. 1979). This is important for CO_2 molecules having a long length.

From a knowledge of the CO_2 orientation, it is possible to determine the CO_2 content of other cordierite samples from their spectra and to construct a working curve for a Raman-based determination of CO_2 concentrations. An orientation with a crystallographic plane containing the X-axis must be used because of the orientation of the CO_2 molecule. To avoid the difficulties associated with the measurement of absolute Raman mode intensities, we ratioed the intensity of the CO_2 stretching mode to a lattice vibration mode. Figure 2 shows the angular dependence of the intensity ratio of the CO_2 stretch at 1383 cm⁻¹ vs. the bands at 973 and 1185 cm⁻¹ in the XY and XZ crystallographic planes. The two latter bands are also observed in XX Raman spectra (Fig. 1) and can be assigned to SiO_4 stretching modes. Both mode intensity ratios are approximately constant in the angular range between X – 30° and X + 30° and may, therefore, be used for this analytical measurement. For the determination of CO_2 contents, the XX spectra of the Sri Lanka cordierite and the six additional cordierites, whose CO_2 content were previously determined (Vry et al. 1990), were measured (Fig. 3). Figure 4 shows the normalized intensities I(1383 cm⁻¹)/I(973 cm⁻¹) and I(1383 cm⁻¹)/I(1185 cm⁻¹) vs. CO_2 content. A reasonable linear trend is apparent. The scatter, we believe, could be related to uncertainties in the determination of the CO_2 or to local differences in CO_2 contents. Vry et al. (1990) determined the CO_2 concentrations from bulk measurements, while we made measurements at a high spatial resolution on a single small cordierite chip. From the curves we can determine the CO_2 content of the Sri Lanka cordierite, for example, as being rather low with about 0.4 wt%.

Internal mode assignments and classification of the different H_2O types

Two types of H_2O were previously identified and described in the literature. Type I and Type II H_2O are distinguished by the orientation of their H··H vectors, which are either parallel or perpendicular to [001], respectively. This classification cannot, however, be carried over into this study for reasons that will be described below. Therefore, we present a new classifi-
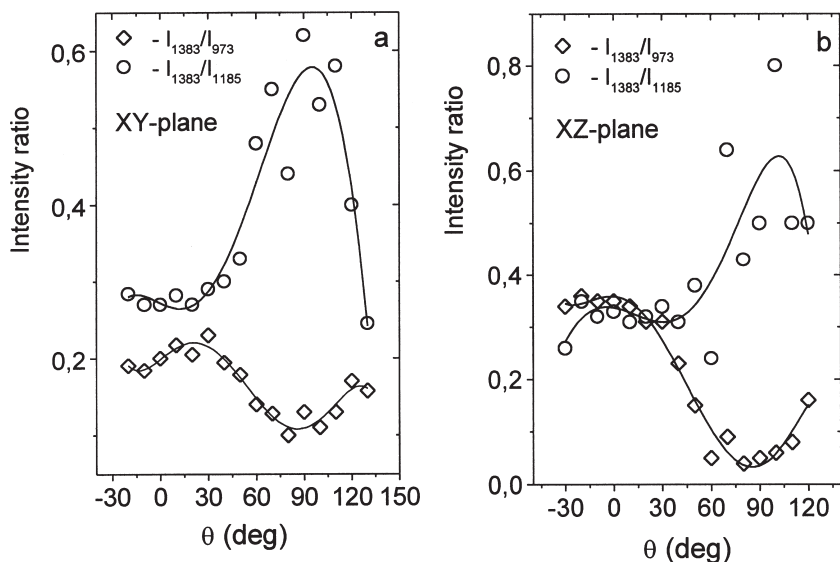
FIGURE 2. The change of the intensity ratio of the CO_2 band at 1383 cm^{-1} and the bands at 973 cm^{-1} and 1185 cm^{-1} (**a**) in XY and (**b**) XZ crystallographic planes.

cation scheme, which is constructed as follows: Two Classes, I and II, of H_2O are described. In the former are placed all types of H_2O molecules that are located in the channel cavity at about 0,0,1/4 and that are not bonded to or have measurable interactions with cations located at 0,0,0 in the six-membered tetrahedral rings. In the second case, Class II, we place all types of H_2O molecules which have some kind of interaction with a channel cation. We describe three types of Class I H_2O and two types of Class II H_2O in cordierite. Our scheme is based on the following observations and analysis.

The alkali-poor cordierites (Sri Lanka and Madagascar) only show a single ν_1 Raman mode at 3597 cm^{-1}, whereas the alkali-containing-samples (Dolni Bory and Haddam) have two ν_1 modes at 3597 and 3578 cm^{-1} in varying intensity ratios (Fig. 5). The Haddam sample, with more Na, has a more intense band at 3578 cm^{-1}. An asymmetric ν_3 mode at higher wave numbers is not observed at room temperatures. A band at about 3597 cm^{-1} is also observed in our polarized IR spectra (Fig. 6) as a weak feature or shoulder in the X, Y, and Z spectra, whereas a stronger ν_1 band at 3575 cm^{-1} is observed in the Z spectrum and appears as a weak shoulder in the X and Y spectra. We assign these two ν_1 modes to H_2O molecules belonging to Class I (~3597 cm^{-1}) and Class II (~3578 cm^{-1}) H_2O. (Fig. 6 is similar to the spectra in Fig 7. of Goldman et al. (1977) for a cordierite from Manitouwadge, Canada.) In the IR spectrum with the electric vector parallel to the Z axis (E‖Z) three strong bands are present at 3575 and 3683 and 3696 cm^{-1}. The latter two are ν_3 vibrations. In the spectrum with E‖Y a broad band at about 3633 cm^{-1} is observed and in the E‖X spectrum a number of weak bands are seen, but the most important is the strongest at 3708 cm^{-1}. At low temperatures, the XZ and YZ Raman spectra resolve bands at 3694 and 3691 cm^{-1}, respectively, in the Dolni Bory and Sri Lanka cordierites (Figs. 7 and 8). They are ν_3 modes having their ν_1 counterparts at ~3597 cm^{-1}, because they lie at wavenumbers about 100 cm^{-1} higher. They are extremely weak or not present in the Raman at room temperatures. They define the Class I-Type I and Class I-Type II
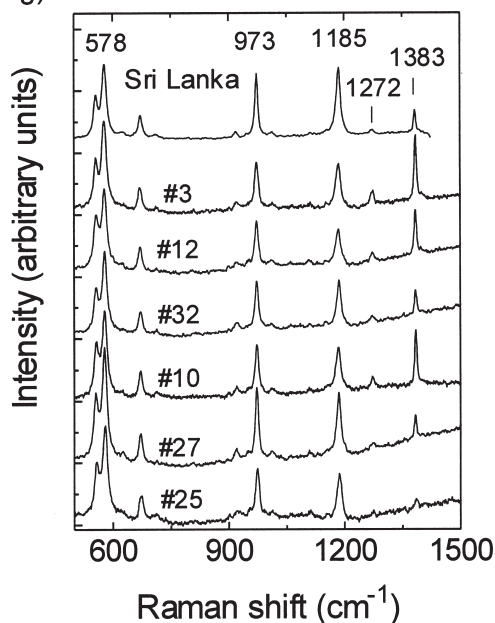

FIGURE 3. Room temperature XX-Raman spectra of the cordierite from Sri Lanka and the six cordierite samples investigated by Vry et al. (1990). The numbers of the samples correspond to those listed in their Table 1.

molecules, respectively. These two different ν_3 modes are intense and slightly more separated in energy in the IR at room temperature in the Mg-rich Sri Lanka cordierite (Fig. 6), where both occur in the Z spectrum at 3696 and 3683 cm^{-1}.

The infrared X spectrum (Fig. 6) shows a moderately strong, sharp band at 3708 cm^{-1} that is not observed in any of the Raman spectra. This is a "new" ν_3 mode not described before, but it is observable in some previously published spectra (see Fig. 7 of Goldman et al. 1977). It is assigned to a new type of H_2O. It should not be associated with any alkali cation, because it is
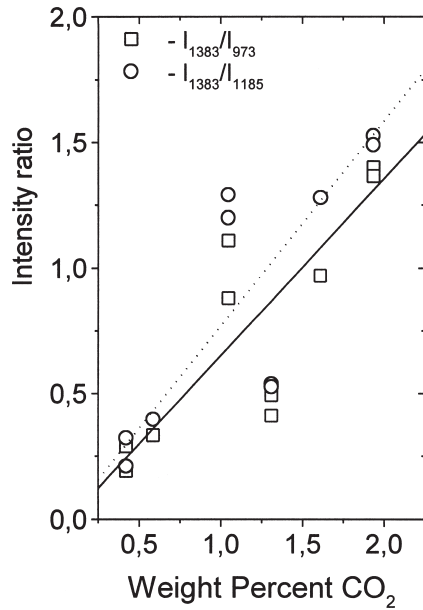
FIGURE 4. The dependence of the I_{1383}/I_{973} (squares) and I_{1383}/I_{1185} (circles) band intensity ratios vs. the CO_2 content (as determined by Vry et al. 1990). The solid and dotted lines are linear least-squares best fits to the two data sets.
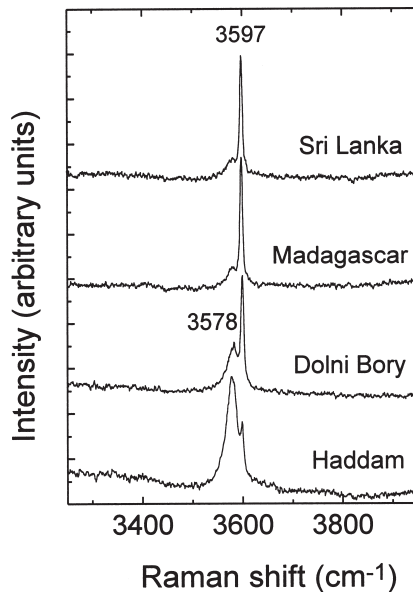
found in the Sri Lanka cordierite and because it is located at high wavenumbers. It is assigned to Class I-Type III H_2O. This band has a narrow FWHH and it could be argued that it is an OH^- stretching mode. From our data, this possibility can not be ruled out. There could exist crystallographically orientated OH^- groups in the cordierite framework (Sugiura 1959) or there could be oriented microscopic OH^- bearing phases in the sample. Its ν_1 counterpart is difficult to define because it will be very weak, but it should lie around 3595 cm^{-1} as in the case of the other two types of Class I H_2O. This Type III should be most stable in the XZ plane, because the channel cavity is longer along the X direction.

As for Class II H_2O, two different ν_3 modes overlap producing a broad band at about 3630 cm^{-1} in both the Raman (Figs. 7 and 8) and IR spectra (Fig. 6) at room temperature. In the Raman at 5K, though, the resolution is better and two components at 3626 and 3639 cm^{-1} are observed. The intensity of this composite band is related to the amount of alkali cations and is stronger in the Dolni Bory spectrum compared to that of Sri Lanka. They are seen in both XZ and YZ spectra, but their intensity in YZ is approximately five times larger than in XZ. They are present in the IR as an asymmetric broad band at ~3633 cm^{-1} in the Y spectrum and a weak broad band at ~3629 cm^{-1} in the X spectrum. From this information, we define a Class II-Type I H_2O as having a ν_3 mode at 3626 cm^{-1} and a Class II-Type II H_2O as having a ν_3 mode at 3639 cm^{-1} (at 5 K). The two ν_1 counterparts are difficult to differentiate, but they are around 3571 cm^{-1} at 5 K and 3575 cm^{-1} at room temperature.

Table 2 classifies the different ν_3 and ν_1 H_2O stretching bands and gives their wave numbers for the IR and Raman spectra at room temperature and 5 K. It also shows the H_2O orientations

FIGURE 5. Room temperature polarized YY single-crystal Raman spectra showing the symmetric mode, ν_1, of the four cordierites of Table 1 in the energy range of the H_2O stretching vibrations.
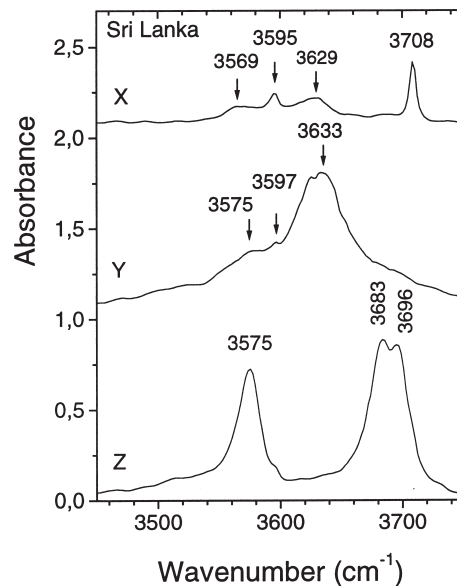

FIGURE 6. Room temperature polarized single-crystal IR absorption spectra of the Sri Lanka cordierite in the energy range of the H_2O stretching vibrations.
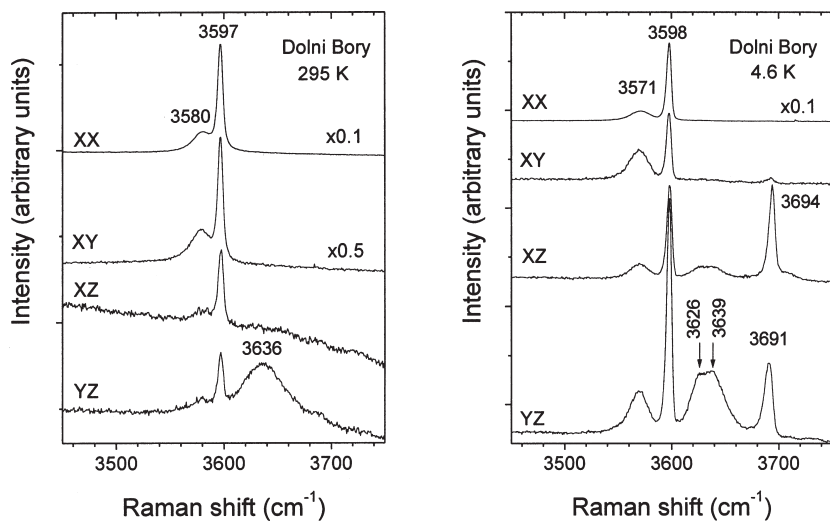
FIGURE 7. Polarized single-crystal Raman spectra of the Dolni Bory cordierite in the energy range of the H_2O stretching vibrations at room temperature (left) and 5 K (right).
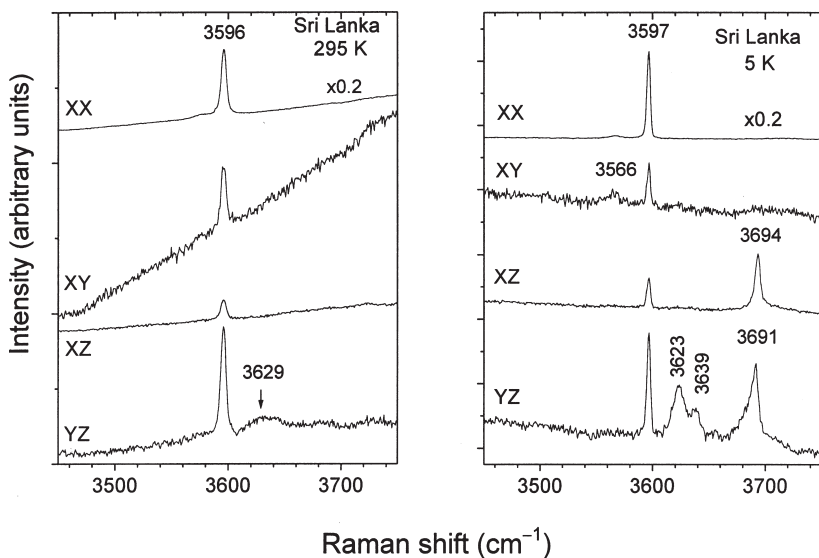

FIGURE 8. Polarized single-crystal Raman spectra of the Sri Lanka cordierite in the energy range of the H_2O stretching vibrations at room temperature (left) and 5 K (right).

for each type relative to the orthorhombic crystal axes as discussed below.

The orientations of Class I—Types I, II, and III H_2O

In theory, the orientation of H_2O can be determined unambiguously from its IR spectra, because the polarization of the v_3 mode gives the direction of the H··H vector and the polarization of the v_1 mode the orientation of the molecular plane. However, the problem of determining the H_2O orientation using IR spectra alone is difficult in practice to solve, because v_1 is very weak or not observed for a free molecule, at least not at room temperature. This is true for Class I H_2O in cordierite and is the same in beryl (Kolesov and Geiger 2000). One needs information from the Raman active modes, in addition, to obtain a complete description of the internal molecular vibrations. In the Raman, the intensity of the v_1 mode along the X, Y, and Z axes

defines the H··H direction, while the polarization direction of the v_3 mode gives the orientation of the molecular plane. So, for example, the angular dependencies of the Raman intensity of the v_1 mode at 3597 cm^{-1} at room temperature for the Sri Lanka cordierite (Fig. 9) show that no Class I H_2O molecules are inclined with respect to any crystallographic axis. Their molecular planes coincide with the those of the crystal. This relationship probably holds for cordierites, but it is not the case in synthetic alkali-free beryl (Kolesov and Geiger 2000).

For Class I Types I and II H_2O, therefore, their H··H vectors are parallel to the channel axis (i.e., [001]) and the molecules lie in the XZ and YZ crystallographic planes, respectively (Figs. 7 and 8). These two types of H_2O alone cannot explain, however, the intensity distribution of the v_1 mode at 3597 cm^{-1} along the X, Y, and Z axes that are 630 (I_{XX}), 920 (I_{YY}), and 1420 (I_{ZZ}) in arbitrary units, respectively (Fig. 9). The first derivatives of
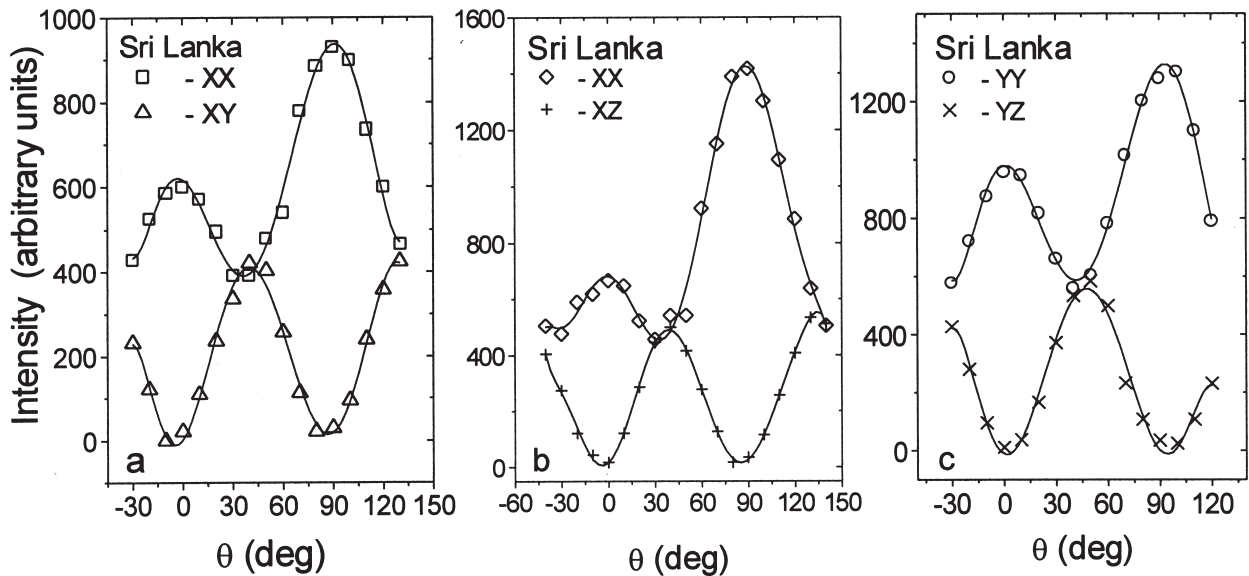
FIGURE 9. Angular dependence of the intensity of the ν_1 Raman mode at 3597 cm^{-1}. The θ-angle is measured (**a**) from the X to the Y axis, (**b**) from the X to the Z axis, and (**c**) from the Y to the Z axis. This shows both parallel and cross polarization of the incident and scattered light relative to the different crystallographic planes. That is, the Raman intensity was measured as the crystal was rotated in about 10° steps in a given crystallographic plane XY or XZ (we use capital letters to denote the crystal axes and small ones the H_2O molecular axes). These spectra give the intensity of the ν_1 mode along the three crystallographic axes.

the polarizability, α'_{ii} (i = x, y, z), of ν_1 for a free H_2O molecule are 10.3 (α'_{xx}), 6.2 (α'_{yy}), and 15.1 (α'_{zz}) (Murphy 1977 and 1978; Raeymaekers et al. 1988), where the x-molecular axis is parallel to the H··H vector, the y-axis perpendicular to the molecular plane, and the z-axis parallel to the C_2 axis of the molecule. An analysis (where one needs to remember that the Raman intensity is proportional to the square of α'_{ii}) shows that there could be at least one additional kind of Class I H_2O and it should have its H··H vector directed along the X axis and its molecular plane in the XZ plane of the crystal. Indeed, the infrared spectra show a band at 3708 cm^{-1} in the X spectrum, as well as a very weak ν_1 shoulder at ~3595 cm^{-1} in the Z spectrum. These two IR bands can be assigned to this "new" sort of H_2O, i.e., Class I-Type III H_2O in cordierite. This is a static description based on the vibrational (Raman and IR) spectra. The possible dynamics will be discussed below.

In summary, Class I H_2O contains three different types of H_2O in the channel cavity. They are characterized by ν_3 modes at 3683, 3696, and 3708 cm^{-1} in Mg-rich alkali-poor cordierite (Table 3) at room temperature and they should have ν_1 modes around 3596 cm^{-1}. The exact wave number for the ν_1 mode of each H_2O Type is, however, difficult to specify and this is an estimate. The reasons governing the temperature dependence of the Raman stretching modes are more complicated and this question will also be discussed below. First, however, the orientation of the second Class of H_2O molecules will be discussed.
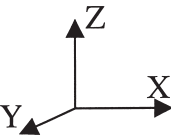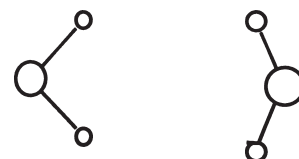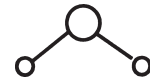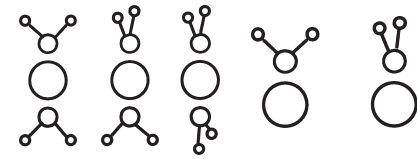
Orientation of Class II—Types I and II H_2O

Class II H_2O, by definition, interacts with an alkali metal centered in the six-membered ring at 0,0,0. The unbonded va-

lence-shell electrons of oxygen in H_2O that determine the bonding properties of a free H_2O molecule are bonded to the alkali cations in this case. The H··H vector of Class II H_2O in the alkali-poor Sri Lanka sample is directed along Y (Fig. 6). Its molecular plane lies in the YZ crystal plane and little to no molecules are in the XZ plane (Fig. 8). In the case of the Dolni Bory cordierite the "double" ν_3 mode is observed in the YZ and XZ Raman spectra and is approximately 5 times more intense in the YZ spectrum (Fig. 7). The two components that are located at 3626 and 3639 cm^{-1} at 5 K maintain the same relative intensities when the polarization direction is changed from YZ to XZ. The two modes are classified as belonging to different Types I and II of H_2O, because of their different energies. Each type has, however, two possible molecule orientations in the YZ and XZ planes at least for the Dolni Bory sample. We did not observe different energies of the ν_3 modes for the different molecular orientations. Hence, unlike Class I Type I/II H_2O, we classify the two sorts only into Types I and II. The FWHH of the 3639 cm^{-1} mode is about 20 cm^{-1} and the other at 3626 cm^{-1} is about 11 cm^{-1} in the Dolni Bory spectrum as determined by fitting them with Lorenzian peaks. The modes in the Sri Lanka spectrum are similar. We assign the higher energy mode to a configuration Type II, in which superimposing H_2O molecules in different channel cavities interact with one alkali cation (Table 2). The lower energy band is assigned to a Class II-Type I orientation where just one H_2O molecule and a neighboring alkali cation interact (Table 2). Kinematic coupling between H_2O molecules may determine the larger band width of the Type II H_2O. We state that both types may have at least two different molecular orientations (XZ and YZ planes).

TABLE 2. Wavenumber (in cm^{-1}), symmetry and assignment of the internal stretching modes of the H_2O molecules in the static description

		Class I			Class II	
		Type 1	Type 2	Type 3	Type 1	Type 2
ν_1	IR*	~3595 (RT)	~3595 (RT)	~3595 (RT)	3575 (RT)	3575 (RT)
	Raman *	~3597 (RT)	~3597 (RT)	~3597 (RT)	3578 (RT)	3578 (RT)
	Raman *	~3598 (5 K)	~3598 (5 K)	~3598 (5 K)	3571 (5 K)	3571 (5 K)
ν_3	IR	3696, Z (RT)	3683, Z (RT)	3708, X (RT)	~3629, X (RT) ~3633, Y (RT)	~3629, X (RT) ~3633, Y (RT)
	Raman	3696 (Sri Lanka)	3691 (Sri Lanka)		3626 (Dolni Bory)	3639 (Dolni Bory)
	Raman	3694 (Dolni Bory) XZ (5 K)	3691 (Dolni Bory) YZ (5 K)		XZ, YZ (5 K)	XZ, YZ (5 K)

* These bands are found in all polarization directions of the crystal axes.

Temperature dependence of the Raman intensity of the ν_3 mode

The intensity of the Raman ν_3 band(s) of Class I-Type I/II H_2O changes dramatically as a function of temperature in cordierite. They are not present at room temperature, but are strong at 5 K. Those of Class II H_2O are observed at both temperatures. These observations are consistent with the different nature of these two Classes of H_2O molecules and their bonding characteristics. Class II H_2O interacts with alkali cations in the six-membered rings, while Class I H_2O is held in place by steric forces at least at room temperature (Wood and Nassau 1968; Winkler et al. 1994a). Hydrogen bonding should be very weak (Langer and Schreyer 1976; Winkler et al. 1994b). The bonding may be different at low temperature. We propose that the reason for the appearance of the ν_3 Raman modes at low temperature is due to the formation of weak hydrogen bonds (see also Kolesov and Geiger 2000, for the case in beryl). It is known that the ν_3 mode of a free H_2O molecule is weakly Raman active and the ν_1 mode is weak in the infrared. Zilles and Person (1983) have shown that a significant increase in ν_1 intensity in the infrared can occur with the formation of a hydrogen bond between two H_2O molecules. The intensity change is related to charge transfer and dynamical polarization of the hydrogen bond along the direction of it. We propose, therefore, that the Raman ν_3 modes of H_2O molecules of Class I Type I and II appear at lower temperatures due to the formation of hydrogen bonds. Very weak hydrogen bonds may occur between the lone electron pairs of the oxygen atoms of the $Si(Al)O_4$ tetrahedra of the six-membered rings and H_2O molecules. Only Class I Types I and II H_2O have the proper orientation to form hydrogen bonds and, therefore, only they exhibit an increase in their ν_3 Raman mode intensities at low temperature. Class I-Type III H_2O that has its H···H vector aligned parallel to the X axis cannot form hydrogen bonds. Therefore, its ν_3 mode is only observed in the infrared (at 3708 cm^{-1}) and not in the Raman at any temperature. Class II H_2O, with its H···H vector perpendicular to [001],

has an orientation which does not allow hydrogen bonds to be formed. This is because the lone electron pairs of the O atoms of the tetrahedra in the center of the cavity wall are directed away from the cavity and cannot bond with the hydrogen atoms. Hence, there is little or no change in their ν_3 mode intensity with decreasing temperature.

Dynamic aspects and analytical determinations of H_2O in cordierite

Much has been written in the literature about the nature of H_2O in cordierite. The original IR work assumed at static state for both Classes (formerly types) of H_2O based on measurements made at room temperature and 77 K (Goldman et al. 1977). At higher temperatures Aines and Rossman (1984) proposed that H_2O begins to enter a free isotropic unbound state. The inelastic neutron scattering data suggest that Class I-Type I/II H_2O (Type I in the older notation) is rotationally disordered (Winkler et al. 1994b). An analysis on natural cordierites is complicated. Winkler (1996) has summarized and discussed the state of affairs and his interpretations can be updated based on our results. For Class I-Type I/II H_2O the molecule flips or hops (residing in each orientation for a few picoseconds) around [001] about its center of mass down to at least 3 K. Our IR and Raman measurements show that two states of the H_2O can occur (i.e., Class I Type I and Type II orientations) as defined by the time scales of the IR and Raman experiment. In both the residence time is long enough to see orientations of the molecule in the YZ and ZX crystal planes (Table 2). In the dynamic model there is no real difference between Class I Types I and II H_2O, although the Type II orientation may have a slightly lower potential energy. Only one type of H_2O is present (i.e., Class I-Type I/II), which is rotationally disordered. It is not clear at this time how Class I-Type III H_2O fits into this picture, as we have too little data to make any clear statements. If it is involved in this dynamic process, then disorder within the channel cavity for Class I H_2O is isotropic

(see Carson et al. 1982) and not simply anisotropic as based on the measurements of pure synthetic Mg-cordierite with only Class I-Type I/II H_2O (Winkler and Hennion 1994). It should be stated here that the rotational disorder in cordierite is different than that in beryl because of the orthorhombic distortion in the former.

There are no inelastic neutron scattering measurements on Class II H_2O and, therefore, an understanding of its dynamic behavior is more difficult to ascertain. The Raman results indicate that the H_2O molecule here can have, as well, two orientations in both the XZ and YZ crystal planes, but with the latter preferred. It is logical to propose that this Class of H_2O may also be dynamically disordered with the molecule jumping between two different orientations. This proposal must be tested, however, with additional measurements.

With regards to the bonding of H_2O in cordierite, some investigators have compared it in a thermodynamic sense to H_2O in water (e.g., Carey and Navrotsky 1992; Newton and Wood 1979), while others have stressed the unbound, anisotropic rotation nature of the molecule at room temperature and lower (e.g., Winkler et al. 1994a). The former consideration implies hydrogen bonding with the cordierite framework, something that is not supported by the spectroscopic and computational data (Langer and Schreyer 1976; Winkler et al. 1994a). Our measurements support the latter interpretation. Class I H_2O in cordierite and beryl could have weak hydrogen bonding at low temperatures, but it is clearly less strong than that in liquid water or ice. It is also clear that the energetics and bonding of Class I Types I and II H_2O are different than those governing Class I Type III H_2O, as demonstrated by the different energies of their ν_3 modes. The experiments of Johannes and Schreyer (1981) and the calculations of Newton and Wood (1979) and Carey (1995) on the thermodynamic state of H_2O in synthetic alkali-free H_2O may not be directly applicable to some natural cordierites, because of the different H_2O types present. All H_2O types must be considered in any thermodynamic treatment of H_2O in natural cordierites. The uncertainty and disagreement in the literature with regard to the more quantitative aspects of the thermodynamics and dynamics of H_2O in cordierite are a result of the complexity of the problem. The "final word" on this is not yet in.

This investigation also demonstrates that previous analytical determinations of the amount of H_2O in cordierite must now be rethought. Bulk methods (e.g., DTA, Karl Fischer titration) or even measurements such as those with an ion-probe will not, in many cases, be able to determine the concentrations of the different molecular types. It is necessary to make spectroscopic measurements, preferably at low temperatures and on single crystals, in order to determine them. Previous H_2O calibrations and determinations need to be rethought. The calibration of Goldman et al. (1977) did not consider the different types of H_2O present. In addition, the effect of CO_2 and alkali cations on the total weight loss of cordierite through heating was not considered.

A final important point is that the interpretations made here through the combined use of IR and Raman spectroscopy, together with the information provided by inelastic neutron scattering measurements, made at different temperatures, show the necessity of undertaking different spectroscopic measurements in order to obtain a complete understanding of the dynamic behavior and orientation of H_2O in cordierite.

REFERENCES CITED

Aines, R.D. and Rossman, G.R. (1984) The high temperature behavior of water and carbon dioxide in cordierite and beryl. American Mineralogist, 69, 319–327.

Ambruster, T. (1985) Ar, N₂, and CO₂ in the structural cavities of cordierite, an optical and X-ray single-crystal study. Physics and Chemistry of Minerals, 12, 233–245.

———(1986) Role of Na in the structure of low-cordierite: A single-crystal X-ray study. American Mineralogist, 71, 746–757.

Ambruster, T. and Bloss, F.D. (1982) Orientation and effects of channel H₂O and CO₂ in cordierite. American Mineralogist, 67, 284–291.

Ambruster, T. and Bürgi, H.B. (1982) Orientation of CO₂ in cavity of cordierite: a single crystal X-ray study at 100 K, 300 K and 500 K. Fortschr. Miner., 60, Beiheft 1, 37–39.

Carey, J.W. (1995) A thermodynamic formulation of hydrous cordierite. Contributions to Mineralogy and Petrology, 119, 155–165.

Carey, J.W. and Navrotsky, A. (1992) The molar enthalpy of dehydration of cordierite. American Mineralogist, 77, 930–936.

Carson, D.G., Rossman, G.R., and Vaughan, R.W. (1982) Orientation and motion of water molecules in cordierite: a proton nuclear magnetic resonance study. Physics and Chemistry of Minerals, 8, 14–19.

Cohen, J.P., Ross, F.K., and Gibbs G.V. (1977) An X-ray and neutron diffraction study of hydrous low cordierite. American Mineralogist, 62, 67–78.

Farrell, E.F. and Newnham R.E. (1967) Electronic and vibrational absorption spectra in cordierite. American Mineralogist, 52, 380–388.

Fredin, L., Nelander, B., and Ribbegard, G. (1977) Infrared spectrum of the water dimer in solid nitrogen. Journal of Chemical Physics, 66, 4065–4072, 4073–4077.

Geiger, C.A., Armbruster, T., Khomenko, V., and Quartieri, S. (2000) Cordierite I: The coordination of Fe²⁺. American Mineralogist, 85, 1255–1264.

Goldman D.S., Rossman, G.R., and Dollase, W.A. (1977) Channel constituents in cordierite. American Mineralogist, 62, 1144–1157.

Hochella, M.F., Brown, G.E., Ross, F.K., and Gibbs, G.V. (1979) High-temperature crystal chemistry of hydrous Mg- and Fe-cordierites. American Mineralogist, 64, 337–351.

Johannes, W. and Schreyer, W. (1981) Experimental introduction of CO₂ and H₂O into Mg-Cordierite. American Journal of Science, 281, 299–317.

Kolesov, B.A. and Geiger, C.A. (2000) The orientation and vibrational states of H₂O in synthetic alkali-free beryl. Physics and Chemistry of Minerals, in press.

Langer, K. and Schreyer, W. (1976) Apparent effects of molecular water on the lattice geometry of cordierite: a discussion. American Mineralogist, 61, 1036–1040.

Le Breton, N. and Schreyer, W. (1993) Experimental CO₂ incorporation into Mg-cordierite: nonlinear behaviour of the system. European Journal of Mineralogy, 5, 427–438.

Murphy, W.F. (1977) The ro-vibrational Raman spectrum of water vapour ν₂ and 2ν₂. Molecular Physics, 33, 1701–1714.

———(1978) The rovibrational Raman spectrum of water vapour ν₁ and ν₃. Molecular Physics, 36, 727–732.

Nelander, B. (1985) Impurity perturbations of the fundamental band of carbon monoxide in solid nitrogen. Journal of Physical Chemistry, 89, 827–830.

Newton, R.C. and Wood, B.J. (1979) Thermodynamics of water in cordierite and some petrologic consequences of cordierite as a hydrous phase. Contributions to Mineralogy and Petrology, 68, 391–404.

Raeymaekers, P., Figeys, H., and Geerlings, P. (1988) Ab initio calculations of the Raman intensities of fundamental vibrations of polyatomic molecules using the improved virtual orbital technique. Journal of Molecular Structure (Theoretical Chemistry), 169, 509–530.

Redington, R.A. and Milligan, D.E. (1962) Infrared spectroscopic evidence for the rotation of the water molecule in solid argon. Journal of Chemical Physics, 37, 2162–2166.

Shannon, R.D., Marinao, A.N., and Rossman, G.R. (1992) Effect of H₂O and CO₂ on dielectric properties of single-crystal cordierite and comparison with polycrystalline cordierite. Journal of the American Ceramic Society, 75, 2395–2399.

Sugiura, K. (1959) The water problem of cordierite. Bulletin of the Tokyo Institute

of Technology, Series-B, no. 1, 1–26.

Tso, T.-L. and Lee, E.K.C. (1985) Role of hydrogen bonding studied by the FTIR spectroscopy of the matrix-isolated molecular complexes, dimer of H$_2$O, H$_2$O·CO$_2$, H$_2$O·CO, and H$_2$O$_2$·nCO in solid O$_2$ at 12-17 K. Journal of Physical Chemistry, 89, 1612–1618.

Vry, J.K., Brown, P.E., and Valley, J.W. (1990) Cordierite volatile content and the role of CO$_2$ in high-grade metamorphism. American Mineralogist, 75, 71–88.

Winkler, B. (1996) The dynamics of H$_2$O in minerals. Physics and Chemistry of Minerals, 23, 310–318.

Winkler, B. and Hennion, B. (1994) Low temperature dynamics of molecular H$_2$O in bassanite, gypsum and cordierite investigated by high resolution incoherent inelastic neutron scattering. Physics and Chemistry of Minerals, 21, 539–545.

Winkler, B., Milman V., and Payne, M.C. (1994a) Orientation, location, and total energy of hydration of channel H$_2$O in cordierite investigated by ab-initio total energy calculations. American Mineralogist, 79, 200–204.

Winkler, B., Coddens, G., and Hennion, B. (1994b) Movement of channel H$_2$O in cordierite observed with quasi-elastic neutron scattering. American Mineralogist, 79, 801–808.

Wood, D.L. and Nassau, K. (1967) Infrared spectra of foreign molecules in beryl. Journal of Chemical Physics, 47, 2220–2228.

——(1968) The characterization of beryl and emerald by visible and infrared absorption spectroscopy. American Mineralogist, 53, 777–800.

Zilles, B. and Person, W.B. (1983) Interpretation of infrared intensity changes on molecular complex formation. I. Water dimer. Journal of Chemical Physics, 79, 65–77.